



Boosting activity of high-fidelity CRISPR/Cas9 variants using a tRNA^{Gln}-processing system in human cells

Received for publication, January 30, 2019, and in revised form, April 11, 2019. Published, Papers in Press, April 22, 2019, DOI 10.1074/jbc.RA119.007791

Xiubin He^{‡S¶}, Yufei Wang^{‡S¶}, Fayu Yang^{‡S¶}, Bang Wang^{‡S¶}, Haihua Xie^{‡S¶}, Lingkai Gu^{‡S¶}, Tianyuan Zhao^{‡S¶},
Xixie Liu^{‡S¶}, Dingbo Zhang^{||**}, Qianwen Ren^{‡S¶}, Xiaoyu Liu^{‡S¶}, Yong Liu^{‡S¶}, Caixia Gao^{||}, and Feng Gu^{‡S¶1}

From the [‡]School of Ophthalmology and Optometry, Eye Hospital, Wenzhou Medical University, Wenzhou, Zhejiang 325027, China, the [§]State Key Laboratory and Key Laboratory of Vision Science, Ministry of Health, Wenzhou, Zhejiang 325027, China, the [¶]Zhejiang Provincial Key Laboratory of Ophthalmology and Optometry, Wenzhou, Zhejiang 325027, China, the ^{||}State Key Laboratory of Plant Cell and Chromosome Engineering and Center for Genome Editing, Institute of Genetics and Developmental Biology, Chinese Academy of Sciences, Beijing 100101, China, and the ^{**}University of Chinese Academy of Sciences, Beijing 100049, China

Edited by Ronald C. Wek

CRISPR/Cas9 nucleases are widely used for genome editing but can induce unwanted off-target mutations. High-fidelity Cas9 variants have been identified; however, they often have reduced activity, constraining their utility, which presents a major challenge for their use in research applications and therapeutics. Here we developed a tRNA^{Gln}-processing system to restore the activity of multiple high-fidelity Cas9 variants in human cells, including SpCas9-HF1, eSpCas9, and xCas9. Specifically, acting on previous observations that small guide RNAs (sgRNAs) harboring an extra A or G (A/G) in the first 5' nucleotide greatly affect the activity of high-fidelity Cas9 variants and that tRNA-sgRNA fusions improve Cas9 activity, we investigated whether a GN₂₀ sgRNA fused to different tRNAs (G-tRNA-N₂₀) could restore the activity of SpCas9 variants in human cells. Using flow cytometry, a T7E1 assay, deep sequencing-based DNA cleavage activity assays, and HEK-293 cells, we observed that a tRNA^{Gln}-sgRNA fusion system enhanced the activity of Cas9 variants, which could be harnessed for efficient correction of a pathogenic mutation in the *retinoschisin 1 (RS1)* gene, resulting in 6- to 8-fold improved Cas9 activity. We propose that the tRNA-processing system developed here specifically for human cells could facilitate high-fidelity Cas9-mediated human genome-editing applications.

CRISPR/Cas9, a type II system of CRISPR derived from the prokaryotic adaptive immune system, has great potential for genome editing and is under intense investigation at the present time (1, 2). The nuclease activity of *Streptococcus pyogenes* Cas9 (SpCas9), the most widely used nuclease at present, can be

triggered by guide RNA targeting imperfectly matched off-target genomic sites. These off-target effects not only confound interpretation of results in the laboratory but also severely undermine the safety and reliability of clinical applications of the technology (3, 4). To address this issue, various strategies and efforts have been employed to minimize off-target activity, such as direct delivery (ribonucleoprotein complex) (5, 6), tunable systems (intein-inactivated Cas9, light-activated and small-molecule induction of Cas9) (7–9), separate Cas9 binding strategies (paired Cas9 nickases) (10), and truncated sgRNA (small guide RNA)² (11). With the delineation and optimization of Cas9 structure, high-fidelity Cas9 variants have been identified, including SpCas9-HF1, eSpCas9(1.1), HypaCas9, evoCas9, xCas9(3.7), Sniper-Cas9, and SpCas9-NG (12–18).

Recent studies revealed that sgRNA transcribed from the U3 or U6 promoter harboring an extra A or G(A/G) in the first nucleotide of the sgRNA may affect the activity of high-fidelity Cas9 variants (19, 20). Thus, selection of endogenous A/G in the first nucleotide position of the 20-nt target sequence is potentially useful. Additionally, different strategies have been adopted to address the extra nucleotide. The tRNA^{Gly} from rice, expressed as a fusion with the guide sequence that would be processed by RNaseP and RNaseZ, boosted the activity of SpCas9-HF1 and eSpCas9(1.1) (19). Meanwhile, self-processing Hammerhead (HH) ribozymes, which self-cleave at their 3' terminus, have also been used in combination with sgRNA to remove the extra G in mammalian cells (20). Here we investigated whether the perfectly matched GN₁₉ could restore the activity of SpCas9 variants in human cells and sought to identify optimized RNA to achieve high-activity and high-fidelity genome editing mediated by Cas9 variants.

Results

Low relative activity of high-fidelity Cas9 variants

According to previous studies, the activity of high-fidelity Cas9 variants is greatly affected by the presence of an extra 5' terminal nucleotide (G) in the sgRNA after transcription from

Funding was provided by National Key R&D Program of China Grant 2018YFA0107304 (to Y. L.), Natural Science Foundation of China Grant 81201181 (to F. G.), Zhejiang Provincial and Ministry of Health Research Fund for Medical Sciences Grant WKJ2013-2-023 (to F. G.), Science Technology Project of Zhejiang Province Grant 2017C37176 (to F. G.), Wenzhou City Grant Y20140633 (to F. G.), Wenzhou Medical University Grant QTJ12011 (to F. G.), and Eye Hospital at Wenzhou Medical University Grant YNZD201602 (to F. G.). The authors declare that they have no conflicts of interest with the contents of this article.

This article contains Figs. S1–S7 and Tables S1–S15.

¹ To whom correspondence should be addressed: Eye Hospital, Wenzhou Medical University, 270 Xueyuan West Road, Wenzhou, Zhejiang 325027, China. Tel.: 86-577-8883-1367. E-mail: gufenguw@gmail.com.

This is an open access article under the CC BY license.

² The abbreviations used are: sgRNA, small guide RNA; HH, Hammerhead; EGFP, enhanced GFP; PAM, protospacer adjacent motif; indel, insertion or deletion.

Boosting activity of Cas9 variants by tRNA processing

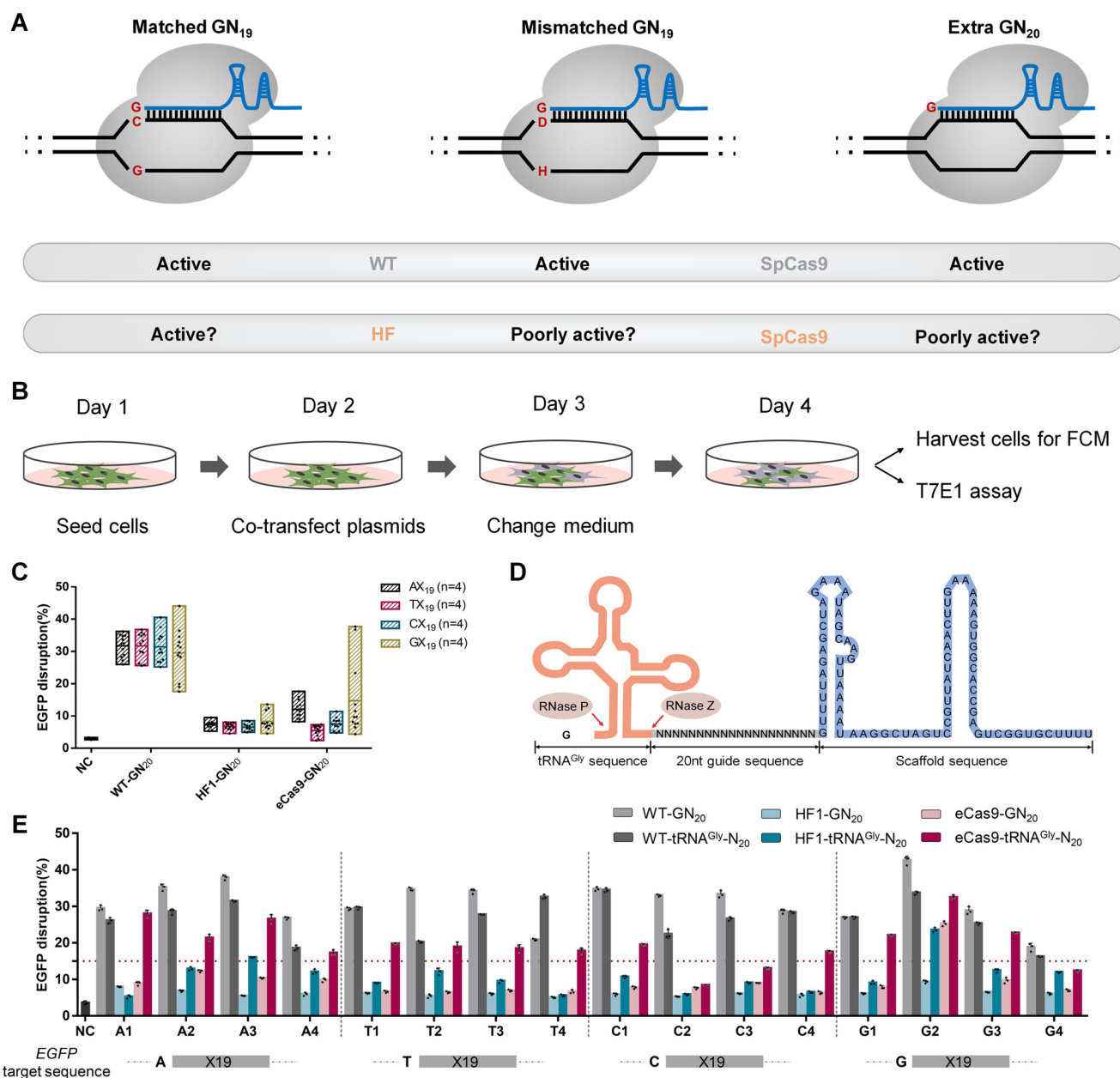


Figure 1. The relatively low activity of high-fidelity Cas9 variants cannot be totally restored with rice tRNA^{Gly}. *A*, schematic of WT Cas9 and variants with three types of sgRNA. The guide sequence is shown in blue. The first nucleotide of the sgRNA or target sequence is shown in red. *A*, A/T/G base; *H*, A/T/C base. *B*, schematic of transfection in 293-SC1 cells. Cas9 and sgRNA expression plasmids are co-transfected into 293-SC1 cells. Transfected cells are harvested for flow cytometry (FCM) or T7E1 assay. *C*, EGFP disruption of Cas9 and variants with GN₂₀ grouped by the first nucleotide of the 20-nt target sequence (AX19, TX19, CX19, and GX19). *D*, schematic of tRNA combined with the sgRNA sequence. tRNA is shown in orange. N₂₀ is shown in gray, and the scaffold sequence is shown in blue. tRNA is cleaved by RNaseP and RNaseZ at the 5' and 3' termini, respectively. *E*, EGFP disruption of Cas9 with GN₂₀ and tRNA^{Gly}-N₂₀ at 16 target sites grouped by the first nucleotide of the 20-nt target sequence (AX19, TX19, CX19, and GX19). Error bars, S.D.; *n* = 3; NC, negative control. GN₂₀ represents the expression sgRNA sequence. AX19, TX19, CX19, and GX19 represent the target sequence.

the U6 promoter. Their performance would be degraded in the presence of the mismatched G, unlike WT SpCas9, which retains its activity (19, 20) (Fig. 1A). Therefore, to confirm whether this is the case, we selected the two most commonly used SpCas9 variants, SpCas9-HF1 (HF1) and eSpCas9(1.1) (eCas9), and used an EGFP reporter cell line (293-SC1), with which it is easy to measure the cleavage activity via flow cytometry (21). We chose 16 target sites in the EGFP gene, grouped by the identity of the first nucleotide (AX19 (sgEGFP-A1~A4), TX19 (sgEGFP-T1~T4), CX19 (sgEGFP-C1~C4), or GX19

(sgEGFP-G1~G4)) and constructed sgRNA expression plasmids of 19 nt (GN₁₉) and 20 nt (GN₂₀) (Fig. S1A and Table S1). For further comparison, coding sequences of WT, HF1, or eCas9 were inserted into the same backbone of pX330. sgRNAs and Cas9 expression plasmids were co-transfected into 293-SC1 cells (Fig. 1B). The results illustrated that HF1 with GN₂₀ possesses no activity at any of the tested sites and that eCas9 with GN₂₀ shows similar results, with the exception of two sites (A2 and G2), which have an activity of 15% and 32%, respectively (Fig. S1B and Fig. 1C). Moreover, compared with the

Boosting activity of Cas9 variants by tRNA processing

activity of GN₂₀ (averaged 7%, HF1-GN₂₀ and averaged 10%, eCas9-GN₂₀), variants with GN₁₉ have higher activity (averaged 15%, HF1-GN₁₉, $p < 0.01$ and averaged 25%, eCas9-GN₁₉, $p < 0.01$). Notably, the activity of WT Cas9 is tolerated over different lengths of the sgRNA sequence (Fig. 1C and Fig. S1C). Unexpectedly, for the perfectly matched sgRNA (GN₁₉) at site G1~G4, notably low activities of Cas9 variants were observed, with the exception of eCas9-GN₁₉ at the G3 site, compared with WT Cas9 (Fig. S1B). Thus, these results, taken together, reveal that the low activity of the Cas9 mutants is not well-restored with the perfectly matched sgRNA (Fig. S1, B and C) in human cells.

It has been reported that tRNA from rice fused with sgRNA (N₂₀) can restore the activity of high-fidelity Cas9 variants in plants (19). The sequence of tRNA^{Gly}-N₂₀ is transcribed from the U6 promoter, which can be recognized by RNaseP and RNaseZ to process the 5' and 3' termini of tRNA, respectively (19) (Fig. 1D). To test whether this strategy works in human cells, we selected 16 sites and found that tRNA does boost Cas9 cleavage activity (HF1-tRNA^{Gly}-N₂₀, averaged 11% versus HF1-GN₂₀, averaged 6% and eCas9-tRNA^{Gly}-N₂₀, averaged 20% versus eCas9-GN₂₀, averaged 9%, Fig. S1D). However, we observed that, at the majority of the sites (13 of 16), high-fidelity Cas9 mutants have much lower activity (approximately averaged 15%), compared with the WT (averaged 27%, Fig. 1E). We also noticed that WT Cas9 combined with tRNA-N₂₀ (averaged 27%) had slightly lower activity than GN₂₀ (averaged 31%) (Fig. S1D). Taken together, the low activity of the high-fidelity Cas9 mutants cannot be restored to WT levels with perfectly matched sgRNA combined with rice tRNA^{Gly} (Fig. 1E and Fig. S1D).

Restoration of the activity of high-fidelity Cas9 variants using a human tRNA-processing system

We reasoned that, because the target cells are of human origin, human tRNA may work better than rice tRNA in improving the activity of high-fidelity Cas9 variants. Also, human tRNA has been utilized to boost the activity of Cpf1 by enhancing the stability of crRNA (CRISPR RNA) for Cpf1 (22). Therefore, we investigated whether human tRNA^{Gln} and tRNA^{Arg}, two of the best-performing tRNAs in Cpf1-mediated genome editing in human cells (22), could be exploited to restore the activity of Cas9 variants. To test this, initially we chose and investigated three sites, sgEGFP-A1~A3. The results revealed that tRNA^{Gln} substantially rescued Cas9 activity at these three sites (16% (tRNA^{Gln}-N₂₀) versus 5% (GN₂₀) at site sgEGFP-A1, 26% versus 7% at site sgEGFP-A2, and 30% versus 3% at site sgEGFP-A3). Our data showed that tRNA^{Arg} possesses lower efficiency than tRNA^{Gln} (Fig. 2, A and B). We then investigated whether tRNA length would affect its efficiency. We tested different lengths (0 nt, 5 nt, 10 nt, 15 nt, and 20 nt) of the upstream sequence of mature tRNA^{Gln} with HF1 at the sgEGFP-A3 site and found that mature tRNA^{Gln} and 5nt-tRNA^{Gln} had the best performance, about 5% higher than others (Fig. 2, A and C). To confirm this, we tested additional target sites with HF1. These results established that different lengths of tRNA (mature tRNA^{Gln} and 5nt-tRNA^{Gln}) were rescued with a comparable efficiency and substantially outperformed tRNA^{Gly} (Fig. S2). As

efficiency with tRNA^{Gln} was slightly higher than 5nt-tRNA^{Gln} with WT Cas9 (Fig. S2), we chose mature tRNA^{Gln} for further study. Testing at additional target sites demonstrated that it did exhibit substantially higher efficiency than tRNA^{Gly}. Specifically, in the case of HF1 with tRNA^{Gln}, the majority (13 of 16) of sites have reasonably high activity (more than 15%) compared with only two sites (2 of 16) with tRNA^{Gly} (Fig. 2, D and E). As for eCas9, encouragingly, with tRNA^{Gln}, the restoration of activity (averaged 32% (tRNA^{Gln}-N₂₀) versus averaged 10% (GN₂₀)) was almost to the same levels as WT Cas9 at all tested sites (Fig. 2, D and E). Collectively, here we demonstrated that a human tRNA-processing system could greatly boost the activity of high-fidelity Cas9 variants.

Effect of a human tRNA-processing system on the activity of xCas9

Recently, xCas9, a high-fidelity Cas9 with a flexible PAM, has been identified (16). We therefore sought to determine whether its activity is the same as WT SpCas9 and whether the effect of a human tRNA processing system would be beneficial. We initially tested xCas9 with EGFP target sites harboring the NGG PAM. The results show that xCas9 has lower activity at all tested sites (Fig. 2F). Similar to the above results, xCas9 with tRNA^{Gln} shows increased activity (Fig. 2G). Specifically, the average efficiency was changed from about 10% (xCas9-GN₂₀) to 21% (xCas9-tRNA^{Gln}-N₂₀) (Fig. 2H). Because it has been reported that xCas9 has flexible PAM selectivity, we tested its activity against 20 EGFP target sites that contain NGT, NGC, NGA, GAN, and NAA PAMs (Fig. S3A and Table S2). Surprisingly, xCas9 showed low activity at all tested sites, even with identical sequences (PAM of TGC, GGA, and GAT) reported in the literature, which claimed higher activity compared with WT Cas9 (Fig. S3B). We could only detect activity at sites with a GGT PAM (Fig. S3B). We then sought to determine whether tRNA^{Gln} is functional combined with xCas9 in noncanonical PAMs in EGFP. No boosting effects were observed, with the exception of the GGT site (35% (tRNA^{Gln}-N₂₀) versus 24% (GN₂₀)) (Fig. 2I).

Taken together, our data show that tRNA^{Gln} has substantially better performance than tRNA^{Gly} in boosting the activity of high-fidelity Cas9 mutants. The ratio of tRNA-N₂₀/GN₂₀ ranged from 0.87 (tRNA^{Gly}) to 1.04 (tRNA^{Gln}) of the WT, 2.79 to 4.54 of HF1, and 3.50 to 5.67 of eCas9 (Fig. S4, A and B). Compared with the WT, the HF1/WT ratio improved from 0.26 (tRNA^{Gly}) to 0.54 (tRNA^{Gln}), and the eCas9/WT ratio improved from 0.60 to 1.03 (Fig. 4, C and D). HF1 and eCas9 with tRNA^{Gln} showed a 4.54-fold and 5.67-fold increase over the parental construct, respectively. In the case of xCas9, tRNA^{Gln} resulted in a 3.58-fold improvement compared with xCas9 (tRNA-N₂₀/GN₂₀) and a 0.62-fold reduction compared with WT Cas9 (Fig. 4, B and D).

Boosting activity with human tRNA processing for correction of a pathogenic mutation

We utilized a 293-RS1 cell line harboring a partial *RS1* coding region carrying a causative mutation (RS1-p.Y65X) from an X-linked juvenile retinoschisis patient (23) (Fig. 3A). Theoretically, EGFP will be expressed when the disease-causing muta-

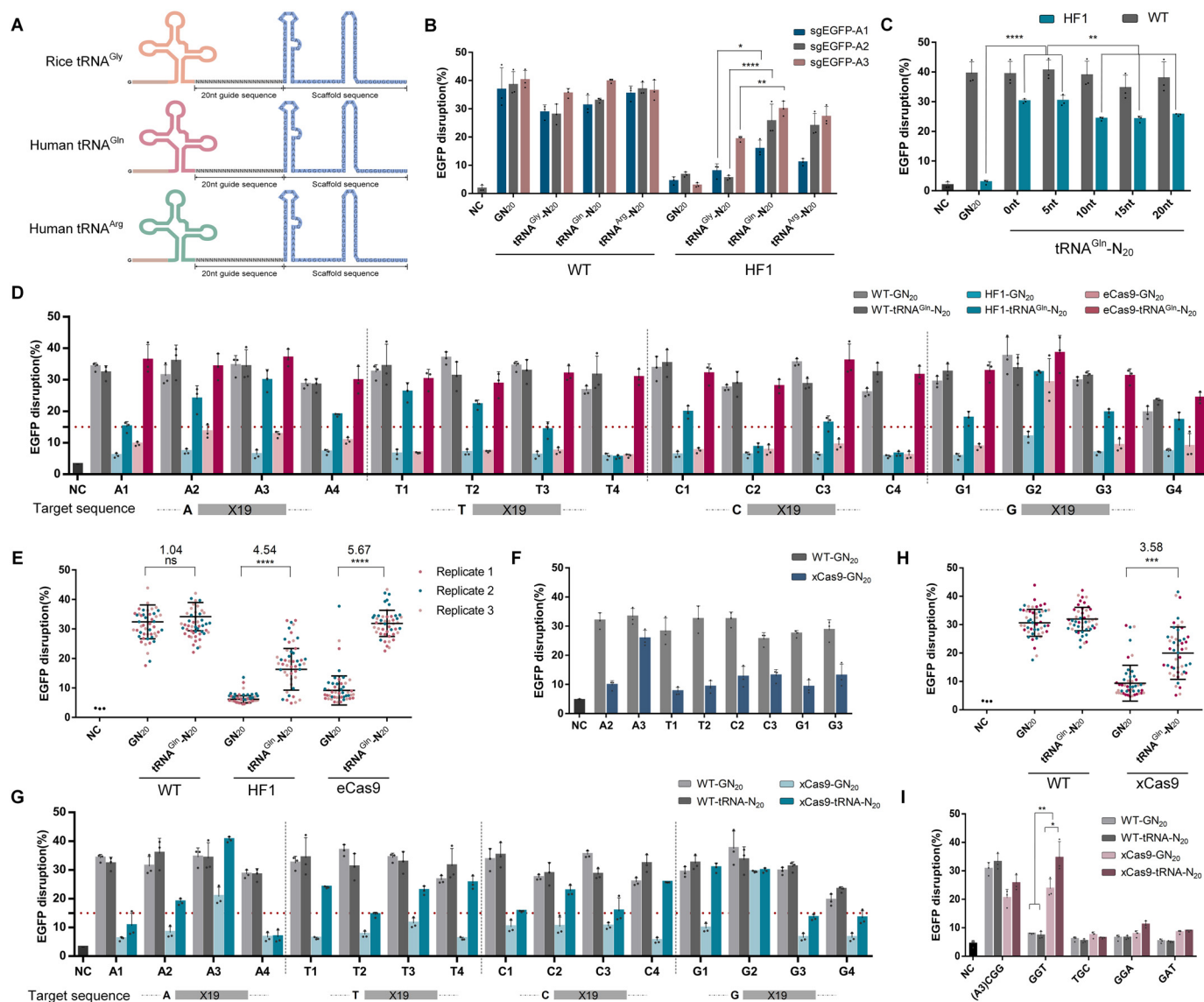


Figure 2. Rescue of Cas9 variant activity with human tRNA. *A*, schematic of different tRNAs (rice tRNA^{Gly}, human tRNA^{Gln}, and human tRNA^{Arg}). *B*, comparison of three tRNAs at sgEGFP-A1, -A2, and -A3 sites. *C*, comparison of different-length (0 nt, 5 nt, 10 nt, 15 nt, and 20 nt) tRNA^{Gln} upstream sequences tested at the A3 site. *D*, EGFP disruption by WT SpCas9 and variants with GN₂₀ and tRNA^{Gln}-GN₂₀ in EGFP disruption. *E*, comparison of the WT and variants GN₂₀ and tRNA^{Gln}-GN₂₀ in EGFP disruption. *F*, EGFP disruption by WT and xCas9 with GN₂₀. *G*, rescue of xCas9 with tRNA^{Gln}-N₂₀ grouped by the first nucleotide of the 20-nt target sequence. *H*, comparison of WT and xCas9, GN₂₀ and tRNA^{Gln}-N₂₀ in EGFP disruption. *I*, EGFP disruption of the non-NGG PAM (GGT, TGC, GGA, GAT) with GN₂₀ and tRNA^{Gln}-N₂₀. Values represent the average ratio of tRNA^{Gln}-N₂₀/GN₂₀ at each site. Error bars, S.D.; *n* = 3; NC, negative control; ns, not significant; *, *p* < 0.05; **, *p* < 0.01; ***, *p* < 0.001; ****, *p* < 0.0001.

tion (stop codon) is removed, generating a novel ORF (when 3 bp indels are generated) of *RS1* (Fig. 3A). We chose two sites (sites 1 and 2) that contain an NGG PAM sequence to test whether human tRNA^{Gln} can boost the activity of WT Cas9 and high-fidelity variants. The results showed that the tRNA had better performance at site 2, which is reasonable for the TAG stop codon to be cleaved at a distance of 3–4 bp from the PAM (Fig. 3, A–C). We observed 6- to 8-fold improved activity of variants compared with GN₂₀, with a 2-fold increase over WT Cas9 at site 2 (Fig. 3C). We also observed the incremental EGFP signal because of tRNA-mediated restoration at site 2 (Fig. 3B). However, nonhomologous end joining cannot perform accurate repair. Therefore, we hypothesized that oligo template-mediated homologous recombination could increase positive EGFP expression. We designed an 86-nt oligo template and

transfected it with Cas9-sgRNA (tRNA^{Gln}-N₂₀) (Fig. 3D). As a result, we detected higher EGFP expression of WT (1.6-fold), HF1 (9.3-fold), eCas9 (1.3-fold), and xCas9 (1.5-fold) with templates than with Cas9-sgRNA alone (Fig. 3E).

Fidelity of WT Cas9 and high-fidelity variants with human tRNA

To investigate whether tRNA would increase or decrease the off-target effects of Cas9, we compared WT Cas9 and its variants with tRNA^{Gln}. We systematically mutated the guide sequence to introduce single mismatches at positions 1 to 20 at site sgEGFP-A3 (Fig. 4A). As before, we co-transfected matched or mismatched tRNA-sgRNAs with Cas9, and EGFP disruption was analyzed by flow cytometry. We transformed the ratio of EGFP disruption of mismatched tRNA-sgRNAs with

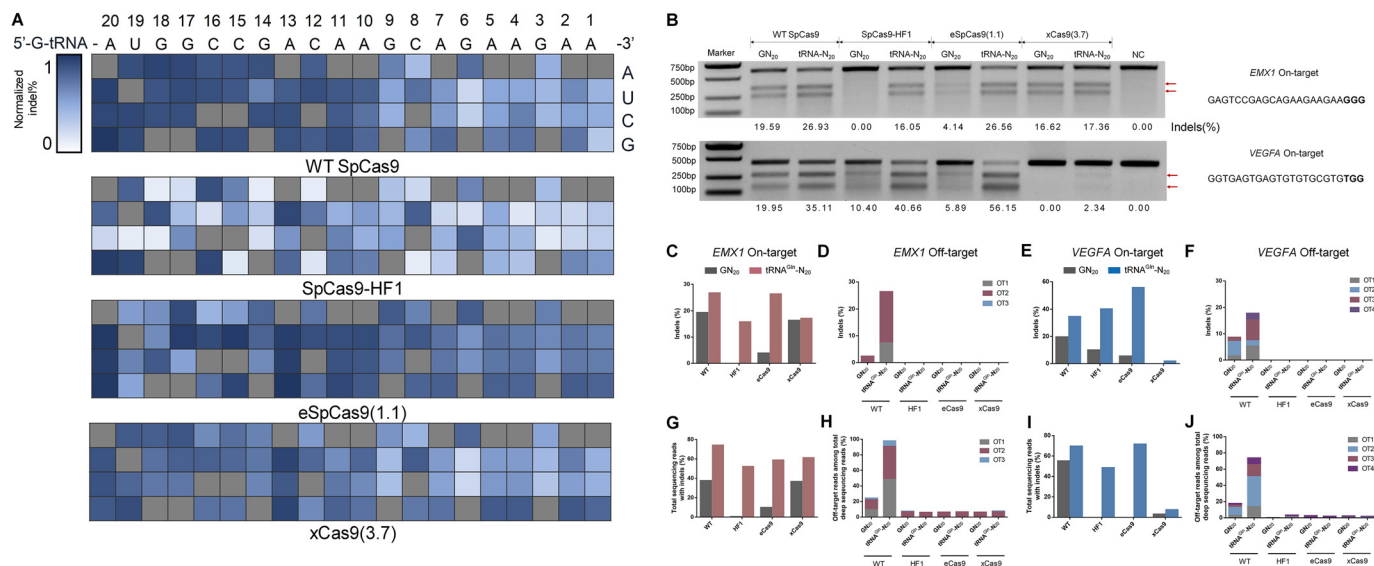


Figure 4. Specificities of Cas9 variants. A, heatmaps showing the indel percentage of the tRNA^{Gln}-N20 sequence with a single-base mismatch at the A3 site. The indel percentage repeated three times is normalized in a range of 0 to 1. The target sequence in heatmaps is shown in gray. B, T7E1 gel image of on-target efficiency at *EMX1* and *VEGFA* sites. The cut size of fragments is indicated by red arrows. The indel percentage is shown below the gels. Target sequences are shown on the right, and the PAM is shown in bold font. C and E, T7E1 analysis of on-target indels at *EMX1* and *VEGFA* sites. D and F, T7E1 analysis of off-target indels at *EMX1* and *VEGFA* sites. G and I, targeted deep sequencing analysis of on-target indels at *EMX1* and *VEGFA* sites. H and J, targeted deep sequencing analysis of off-target indels at *EMX1* and *VEGFA* sites.

WT/HF1/eCas9/xCas9 and matched tRNA–sgRNAs with WT/HF1/eCas9/xCas9 to heatmaps (Fig. 4A). The results revealed that HF1 induced the lowest indel levels among three variants, with notably improved specificity at both the 5' and 3' termini (Fig. 4A and Fig. S5). The other two variants, eCas9 and xCas9, showed slightly reduced activity at off-target sites only at the 5' terminus (Fig. 4A). To further characterize their performance at genomic loci, we chose two endogenous sites in *EMX1* and *VEGFA* (12). As expected, there was a substantial increase in the on-target efficiency of WT, HF1 and eCas9, which was consistent with previous results with the EGFP reporter system. At the *EMX1* site, with tRNA^{Gln}, the cleavage efficiency was increased from 20% (without tRNA^{Gln}) to 27% (with tRNA^{Gln}, WT), 0% to 16% (HF1), and 4% to 27% (eCas9) (Fig. 4, B and C). At the *VEGFA* site, the cleavage efficiency was increased from 20% to 35% (WT), 10% to 41% (HF1), and 6% to 56% (eCas9) (Fig. 4, B and E). In the case of xCas9, with tRNA^{Gln}, relative increased activity or detectable cleavage was observed with *EMX1* and *VEGFA* (Fig. 4, B, C, and E). With tRNA^{Gln}, high-fidelity Cas9 variants had higher activity, and no off-target effects were observed compared with its parentals (Fig. 4, D and F, and Fig. S6). Not surprisingly, we observed notable off-target effects with WT Cas9. To further evaluate the performance of tRNA, we utilized deep sequencing to test on-target sites and off-target sites examined with T7E1. The results revealed a similar outcome that tRNA restored the efficiency of WT, HF1, eCas9, and xCas9. Also, no increasing off-target effects of high-fidelity variants were observed (Fig. 4, G–J). We noticed that the efficiency detected by deep sequencing was almost two times the efficiency observed using T7E1, which is consistent with a previous study showing that T7E1 is not sensitive enough to detect all indels (23) but is still a simple and quick method to test activity and off-target effects.

Discussion

In this study, we demonstrated that the first G nucleotide transcribed from the U6 promoter is extremely important in the activity of Cas9 variants because of their sensitivity to spacer length and mismatch in human cells. Our results also provide direct evidence that there is no apparent regularity of the first nucleotide in the 20-nt target sequence. Curiously, even with a perfectly matched G, there was no benefit for Cas9 variants compared with WT Cas9. Currently, the reasons underlying this observation are not clear, and further studies will dissect the molecular mechanism involved. To rescue the activity of high-fidelity Cas9 variants, we utilized tRNA^{Gly} from rice, which has been reported to boost Cas9 activity in plants (19). However, this approach is inefficient in human cells and even somewhat attenuated the activity of WT Cas9 (13% reduction). We speculate that tRNA processing in plant cells may be different from that in mammalian cells. Therefore, we developed a human tRNA-processing system to rescue the activity of Cas9 variants. We exploited human tRNA^{Gln} and tRNA^{Arg}, which showed improved performance compared with tRNA^{Gly} from rice. However, tRNA^{Gln} behaved moderately better than tRNA^{Arg}. The difference between these nucleotide sequences may underlie the different levels of restoration of Cas9 activity (Fig. S7).

The results illustrated that, in the presence of mature tRNA^{Gln}, Cas9 variant activity was restored to different extents. At *EGFP* target sites, HF1 only recovered an average of 54% activity relative to WT Cas9 compared with almost complete recovery with eCas9 (Fig. S4D). This is consistent with the results observed in endogenous genes (Figs. 3C and 4, B–J). To account for this, we speculate that some mutated residues of HF1 may be involved in RNA–DNA heteroduplex recognition (14), inducing the diminished catalytic activity of Cas9, or per-

Boosting activity of Cas9 variants by tRNA processing

haps there is an interaction between tRNA–sgRNA and RNase that may hinder tRNA processing. Theoretically, after processing, tRNA-N₂₀ of site G1~G4 is perfectly matched with GN₁₉. However, increased Cas9 activity with tRNA-N₂₀ at site G1~G4 has been observed (Fig. 2D). We suspect that tRNA may play another role in structural interactions that enhance Cas9 activity.

Notably, we found that xCas9 is sensitive to the extra G but not to the same extent as HF1. With tRNA processing, xCas9 only recovered about 62% activity of WT Cas9 at NGG PAM sites in EGFP, moderately higher than HF1 (Fig. S4D). The activity of xCas9 with tRNA was maintained at endogenous sites compared with the other two variants. For non-NGG PAM sites, we found that xCas9 possesses rather low activity with sgRNA-GN₁₉, even at the same sites (PAM of TGC, GGA, GAT) tested in the literature, with exception of the GGT site in human cells (Fig. 2I), suggesting that xCas9 may not be as effective with an extended PAM, consistent with recent data (18). In this study, we did not test the HH ribozyme strategy, as for each sgRNA a different HH sequence should be used, which makes construction of sgRNA complicated (20).

Collectively, the human tRNA^{Gln} used in our study provides a new method to restore the activity of high-fidelity Cas9 variants in human cells, which broadens the editing regions for selection of the target sequences. As a tool, tRNA may be applied to additional Cas9 variants, such as evoCas9, HypaCas9, Cas9-NG, or Sniper-Cas9. The human tRNA-processing system enabled development of a promising and applicable approach to genome editing with CRISPR/Cas9 high-fidelity variants.

Experimental procedures

Plasmid constructions

Plasmids pX330 (harboring the WT SpCas9 coding sequence), eSpCas9 (1.1), SpCas9-HF1, and xCas9(3.7)-ABE(7.10) were obtained from Addgene (plasmids 42230, 71814, 72247, and 108382, respectively). To make them comparable, we generated all constructs with the same backbone. Specifically, the coding sequences for SpCas9 from SpCas9-HF1 and xCas9(3.7)-ABE(7.10) were amplified and inserted into the backbone of pX330 (without the SpCas9 coding sequence). The coding sequence of SpCas9 from xCas9(3.7)-ABE(7.10) was in the dead form, which was mutated to the active form with site-directed mutagenesis for this study. sgRNA oligos were annealed and inserted into the backbone of pX330 using a standard protocol. DNA sequencing confirmed the desired specific sequences in the constructs. The oligonucleotide, target, and primer sequences in the present study are summarized in Tables S1–S15.

Cell culture and cell transfection

HEK-293 cells (catalog no. CRL-1573) expressing EGFP were generated by lentiviral transduction as described previously (21). Drug-resistant single colonies of transduced HEK-293 cells were isolated and named 293-SC1. To maintain EGFP expression, the medium for 293-SC1 culture included puromycin. Cells were cultured in advanced DMEM (Life Technologies) supplemented with 10% FBS and 1% penicillin–

streptomycin at 37 °C with 5% CO₂. 1.8 × 10⁵ 293-SC1 cells were seeded per well of a 12-well plate on day 1. The 293-SC1 cells were transfected with 750 ng of plasmids (250 ng of sgRNA and 500 ng of Cas9 expression plasmids) using 3.0 μl of TurboFect (Thermo Fisher Scientific) on day 2. Fresh medium was added to the transfected 293-SC1 cells on day 3. The cells were harvested for flow cytometry, T7 Endonuclease I (T7E1) assay, or deep sequencing on day 4.

DNA cleavage activity assay

The flow cytometry experiments were performed as described previously (21). The background of EGFP disruption was gated at in a range of 1% to 5% for all experiments. Fragments harboring insertions or deletions (indels) were amplified by PCR using the primer sets listed in Table S2. For the T7E1 assay, 300 ng of purified PCR products was mixed with 1 μl of 10 × NEBuffer 2 and ultrapure water to a final volume of 14.5 μl and subjected to a reannealing process to enable heteroduplex formation (24). After reannealing, products were treated with T7 Endonuclease I (New England Biolabs). Quantification was based on relative band intensities. The indel percentage was determined by the formula $100 \times (1 - \sqrt{(b + c)/(a + b + c)})$, where a is the integrated intensity of the undigested PCR product and b and c are the integrated intensities of the cleavage product. Primers and target sequence are summarized in Table S3.

Targeted deep sequencing assay

Genomic regions of interest were amplified by PCR with flanking high-throughput sequencing (HTS) primer pairs that are listed in Table S15. PCR reactions were carried out under the following conditions: 95 °C for 5 min, then 34 cycles of 95 °C for 30 s, 58 °C for 30 s, and 72 °C for 15 s, followed by a final 72 °C extension for 5 min. PCR products were verified on a 2.0% agarose gel and purified using a DNA extraction kit (Vazyme). Purified products were sequenced on an Illumina HiSeq X Ten instrument at Novogene (Tianjin, China). Sequencing data were obtained using standard protocols.

Statistics

All data replicated three times were expressed as mean ± S.D. Differences between two groups were determined by two-tailed Student's *t* test or Mann–Whitney test. The criteria for statistical significance were as follows: **p* < 0.05, ***p* < 0.01, ****p* < 0.001, and *****p* < 0.0001.

Author contributions—X. H. software; X. H., L. G., T. Z., Xiexie Liu, and D. Z. formal analysis; X. H., F. Y., B. W., H. X., L. G., T. Z., Xiexie Liu, Q. R., and Xiaoyu Liu methodology; X. H. writing-original draft; X. H., Y. W., and F. G. project administration; X. H., F. Y., H. X., and F. G. writing-review and editing; F. Y., B. W., H. X., Y. L., and C. G. supervision; F. Y., B. W., and H. X. validation; Y. L. and F. G. funding acquisition; F. G. conceptualization.

Acknowledgments—We thank Xianglian Ge, Xiujuan Lv, Mengjun Tu, Fanfan Li, Huihui Sun, and Jie Liu for technical assistance.

References

- Jinek, M., Chylinski, K., Fonfara, I., Hauer, M., Doudna, J. A., and Charpentier, E. (2012) A programmable dual-RNA-guided DNA endonuclease in adaptive bacterial immunity. *Science* **337**, 816–821 [CrossRef Medline](#)
- Komor, A. C., Badran, A. H., and Liu, D. R. (2017) CRISPR-based technologies for the manipulation of eukaryotic genomes. *Cell* **168**, 20–36 [CrossRef Medline](#)
- Tsai, S. Q., Zheng, Z., Nguyen, N. T., Liebers, M., Topkar, V. V., Thapar, V., Wyvekens, N., Khayter, C., Iafrate, A. J., Le, L. P., Aryee, M. J., and Joung, J. K. (2015) GUIDE-seq enables genome-wide profiling of off-target cleavage by CRISPR-Cas nucleases. *Nat. Biotechnol.* **33**, 187–197 [CrossRef Medline](#)
- Kuscu, C., Arslan, S., Singh, R., Thorpe, J., and Adli, M. (2014) Genome-wide analysis reveals characteristics of off-target sites bound by the Cas9 endonuclease. *Nat. Biotechnol.* **32**, 677–683 [CrossRef Medline](#)
- Kim, S., Kim, D., Cho, S. W., Kim, J., and Kim, J. S. (2014) Highly efficient RNA-guided genome editing in human cells via delivery of purified Cas9 ribonucleoproteins. *Genome Res.* **24**, 1012–1019 [CrossRef Medline](#)
- Kim, K., Park, S. W., Kim, J. H., Lee, S. H., Kim, D., Koo, T., Kim, K. E., Kim, J. H., and Kim, J. S. (2017) Genome surgery using Cas9 ribonucleoproteins for the treatment of age-related macular degeneration. *Genome Res.* **27**, 419–426 [CrossRef Medline](#)
- Davis, K. M., Pattanayak, V., Thompson, D. B., Zuris, J. A., and Liu, D. R. (2015) Small molecule-triggered Cas9 protein with improved genome-editing specificity. *Nat. Chem. Biol.* **11**, 316–318 [CrossRef Medline](#)
- Jain, P. K., Ramanan, V., Schepers, A. G., Dalvie, N. S., Panda, A., Fleming, H. E., and Bhatia, S. N. (2016) Development of light-activated CRISPR using guide RNAs with photocleavable protectors. *Angew. Chem. Int. Ed. Engl.* **55**, 12440–12444 [CrossRef Medline](#)
- Dow, L. E., Fisher, J., O'Rourke, K. P., Muley, A., Kasthuber, E. R., Livshits, G., Tschaharganeh, D. F., Socci, N. D., and Lowe, S. W. (2015) Inducible *in vivo* genome editing with CRISPR-Cas9. *Nat. Biotechnol.* **33**, 390–394 [CrossRef Medline](#)
- Ran, F. A., Hsu, P. D., Lin, C. Y., Gootenberg, J. S., Konermann, S., Trevino, A. E., Scott, D. A., Inoue, A., Matoba, S., Zhang, Y., and Zhang, F. (2013) Double nicking by RNA-guided CRISPR Cas9 for enhanced genome editing specificity. *Cell* **154**, 1380–1389 [CrossRef Medline](#)
- Fu, Y., Sander, J. D., Reyon, D., Cascio, V. M., and Joung, J. K. (2014) Improving CRISPR-Cas nuclease specificity using truncated guide RNAs. *Nat. Biotechnol.* **32**, 279–284 [CrossRef Medline](#)
- Kleinstiver, B. P., Pattanayak, V., Prew, M. S., Tsai, S. Q., Nguyen, N. T., Zheng, Z., and Joung, J. K. (2016) High-fidelity CRISPR-Cas9 nucleases with no detectable genome-wide off-target effects. *Nature* **529**, 490–495 [CrossRef Medline](#)
- Slaymaker, I. M., Gao, L., Zetsche, B., Scott, D. A., Yan, W. X., and Zhang, F. (2016) Rationally engineered Cas9 nucleases with improved specificity. *Science* **351**, 84–88 [CrossRef Medline](#)
- Chen, J. S., Dagdas, Y. S., Kleinstiver, B. P., Welch, M. M., Sousa, A. A., Harrington, L. B., Sternberg, S. H., Joung, J. K., Yildiz, A., and Doudna, J. A. (2017) Enhanced proofreading governs CRISPR-Cas9 targeting accuracy. *Nature* **550**, 407–410 [CrossRef Medline](#)
- Casini, A., Olivieri, M., Petris, G., Montagna, C., Reginato, G., Maule, G., Lorenzin, F., Prandi, D., Romanel, A., Demichelis, F., Inga, A., and Cereseto, A. (2018) A highly specific SpCas9 variant is identified by *in vivo* screening in yeast. *Nat. Biotechnol.* **36**, 265–271 [CrossRef Medline](#)
- Hu, J. H., Miller, S. M., Geurts, M. H., Tang, W., Chen, L., Sun, N., Zeina, C. M., Gao, X., Rees, H. A., Lin, Z., and Liu, D. R. (2018) Evolved Cas9 variants with broad PAM compatibility and high DNA specificity. *Nature* **556**, 57–63 [CrossRef Medline](#)
- Lee, J. K., Jeong, E., Lee, J., Jung, M., Shin, E., Kim, Y. H., Lee, K., Jung, I., Kim, D., Kim, S., and Kim, J. S. (2018) Directed evolution of CRISPR-Cas9 to increase its specificity. *Nat. Commun.* **9**, 3048 [CrossRef Medline](#)
- Nishimasu, H., Shi, X., Ishiguro, S., Gao, L., Hirano, S., Okazaki, S., Noda, T., Abudayyeh, O. O., Gootenberg, J. S., Mori, H., Oura, S., Holmes, B., Tanaka, M., Seki, M., Hirano, H., *et al.* (2018) Engineered CRISPR-Cas9 nuclease with expanded targeting space. *Science* **361**, 1259–1262 [CrossRef Medline](#)
- Zhang, D., Zhang, H., Li, T., Chen, K., Qiu, J. L., and Gao, C. (2017) Perfectly matched 20-nucleotide guide RNA sequences enable robust genome editing using high-fidelity SpCas9 nucleases. *Genome Biol.* **18**, 191 [CrossRef Medline](#)
- Kim, S., Bae, T., Hwang, J., and Kim, J. S. (2017) Rescue of high-specificity Cas9 variants using sgRNAs with matched 5' nucleotides. *Genome Biol.* **18**, 218 [CrossRef Medline](#)
- Zhang, Y., Ge, X., Yang, F., Zhang, L., Zheng, J., Tan, X., Jin, Z. B., Qu, J., and Gu, F. (2014) Comparison of non-canonical PAMs for CRISPR/Cas9-mediated DNA cleavage in human cells. *Sci. Rep.* **4**, 5405 [Medline](#)
- Wu, H., Liu, Q., Shi, H., Xie, J., Zhang, Q., Ouyang, Z., Li, N., Yang, Y., Liu, Z., Zhao, Y., Lai, C., Ruan, D., Peng, J., Ge, W., Chen, F., *et al.* (2018) Engineering CRISPR/Cpf1 with tRNA promotes genome editing capability in mammalian systems. *Cell. Mol. Life Sci.* **75**, 3593–3607 [CrossRef Medline](#)
- Yang, F., Ge, X., He, X., Liu, X., Zhou, C., Sun, H., Zhang, J., Zhao, J., Song, Z., Qu, J., Liu, C., and Gu, F. (2018) Functional non-homologous end joining patterns triggered by CRISPR/Cas9 in human cells. *J. Genet. Genomics* **45**, 329–332 [CrossRef Medline](#)
- Lin, L., He, X., Zhao, T., Gu, L., Liu, Y., Liu, X., Liu, H., Yang, F., Tu, M., Tang, L., Ge, X., Liu, C., Zhao, J., Song, Z., Qu, J., and Gu, F. (2018) Engineering the direct repeat sequence of crRNA for optimization of FnCpf1-mediated genome editing in human cells. *Mol. Ther.* **26**, 2650–2657 [CrossRef Medline](#)